

Article

Treatment of Actual Chemical Wastewater by a Heterogeneous Fenton Process Using Natural Pyrite

Liang Sun, Yan Li and Aimin Li *

State Key Laboratory of Pollution Control and Resources Reuse, School of the Environment, Nanjing University, Nanjing 210023, China; E-Mails: sunliangphd@tju.edu.cn (L.S.); liyan_0921@126.com (Y.L.)

* Author to whom correspondence should be addressed; E-Mail: liaimin@nju.edu.cn; Tel./Fax: +86-25-8968-0377.

Academic Editors: Rao Bhamidimarri and Kiran Tota-Maharaj

Received: 14 September 2015 / Accepted: 20 October 2015 / Published: 28 October 2015

Abstract: Wastewater from chemical plants has remarkable antibiotic effects on the microorganisms in traditional biological treatment processes. An enhanced Fenton system catalyzed by natural pyrite was developed to degrade this kind of wastewater. Approximately 30% chemical oxygen demand (COD) was removed within 120 min when 50 mmol/L H₂O₂ and 10 g/L natural pyrite were used at initial pH from 1.8 to 7. A BOD₅/COD enhancement efficiency of 210% and an acute biotoxicity removal efficiency of 84% were achieved. The COD removal efficiency was less sensitive to initial pH than was the classic Fenton process. Excessive amounts of pyrite and H₂O₂ did not negatively affect the pyrite Fenton system. The amount of aniline generated indicated that nitrobenzene reduction by pyrite was promoted using a low initial concentration of H₂O₂ (<5 mmol/L). Fluorescence excitation emission matrix analyses illustrated that H₂O₂ facilitated the reduction by natural pyrite of organic molecules containing an electron-withdrawing group to electron-donating group. Thus, the Fenton-like process catalyzed by pyrite can remediate wastewater containing organic pollutants under mild reaction conditions and provide an alternative environmentally friendly method by which to reuse natural pyrite.

Keywords: natural pyrite; heterogeneous Fenton process; chemical wastewater; reduction

1. Introduction

Wastewater from chemical plants is a significant source of environmental contamination [1–3]. This kind of wastewater has remarkable antibiotic effects on microorganisms in traditional biological treatment processes because various organic compounds in the wastewater, especially nitro-aromatic compounds such as nitrobenzene, are toxic and bio-refractory [4,5]. Therefore, technologies that improve the biodegradability of this type of wastewater should be developed.

Various methods have been proposed to address this challenge. Physical-chemical technologies have been used to modify the chemical characteristics of wastewaters and render them treatable in biological systems without adverse effects. Advanced oxidation processes, such as Fenton reactions [6,7], ozonation [8,9], and photochemical oxidation [10,11] have shown great potential due to their high efficiency in removing refractory compounds. These technologies can mineralize contaminants completely and have been intensively investigated. In particular, the Fenton reactions have been proven to be one of the best choices for practical application because of their high efficiency, simple operation, and low cost. However, in spite of the high oxidation performance, the classic Fenton reaction (which is catalyzed by soluble Fe^{2+}) has some critical limitations: The operation needs to start under low initial pH (the optimum pH usually is 3) and the stoichiometric quantity of soluble Fe^{2+} that must be added generates significant amounts of sludge [12–14]. In the last few decades, the use of iron-bearing oxides (instead of soluble Fe^{2+}) as heterogeneous catalysts has received increasing attention as a means by which to overcome these drawbacks. Several studies have reported that the use of iron-bearing oxides as catalysts in Fenton reactions has advantages of low cost and easy operation, and may exhibit excellent catalysis performance in the removal of organic contaminants [15–17].

Pyrite (FeS_2) is the most abundant metal sulfide on the surface of Earth [18] and can be an appropriate material to act as a heterogeneous catalyst in the Fenton reaction. For example, Matta and Arienzo used a pyrite Fenton system for the oxidative degradation of 2,4,6-trinitrotoluene and reported that the observed degradation kinetics were much faster than those in the presence of other iron minerals such as magnetite and ferrihydrite [15,19]. Che and Bae used a pyrite Fenton system for the oxidative degradation of trichloroethylene and diclofenac, and reported that the degradation of both compounds was better in the pyrite Fenton system than in a classic Fenton system [20,21]. Wu found that hydrogen peroxide (H_2O_2) enhanced by natural pyrite had great activity in the decoloration of azo dyes [22]. Zhang demonstrated that the degradation of nitrobenzene in the pyrite Fenton system was significantly enhanced compared to that achieved in a classic Fenton system [23].

However, there is little in the literature describing the application of the pyrite Fenton process to treat actual wastewater. The performance of this technology in remediating chemical wastewater is not yet known. Data are needed that define the catalytic performance of the pyrite Fenton process for the treatment of chemical wastewater so that the feasibility and application of this technology can be evaluated.

Meanwhile, reducing the quantity of contaminants may not necessarily be effective in reducing health and environmental risks because some degradation products may be more toxic than their parent compounds [24]. Several examples of this case have been reported in wastewater treatment processes [2,24]. Thus, information on the biodegradability and biotoxicity of chemical wastewater treated using the pyrite Fenton process is essential to evaluating the ecological safety and overall feasibility of this technology.

In the present study, the heterogeneous Fenton process using natural pyrite has been developed. The reactivity performance of the pyrite Fenton system was compared to that of a classic Fenton system when given the same initial conditions (iron content, H₂O₂ concentration, initial pH), and the effects of the dosage of pyrite and H₂O₂ on the removal of chemical oxygen demand (COD) were evaluated in detail. The biodegradability and biotoxicity of the treated wastewater were also assessed. Fluorescence excitation emission matrix (EEM) analysis was used to characterize the change of functional groups in the wastewater before and after treatment using the pyrite Fenton process. The results showed that adding a small quantity of H₂O₂ could enhance the reducing performance of the natural pyrite. The results contribute to a better understanding of the mechanism and reaction process of the pyrite Fenton technology. This report is the first to describe the reduction of nitrobenzene through Fenton oxidation catalyzed by natural pyrite.

2. Experimental Section

2.1. Reagents and Wastewater

Chemicals used in the experiments consisted of reagent grade (AR) H₂O₂ (30%), iron (II) sulfate heptahydrate (FeSO₄·7H₂O), sulfuric acid (H₂SO₄, 98%), hydrochloric acid (HCl), and sodium hydroxide (NaOH) and were obtained from the Sinopharm Chemical Reagent Co. Ltd., Shanghai, China. All chemicals were used without further purification. The pyrite used in the experiments was mined from Anhui, China. The pyrite was sieved to a 300-mesh powder, washed with 1 mol HCl to remove surface oxidation layers, rinsed three times with deoxygenated deionized water and dehydrated with ethanol, and dried and stored in a closed vial under a pure nitrogen atmosphere. Elemental analyses showed that the iron content of the pyrite was 25%. The BET surface area of the pyrite was 5.960 m²/g.

The wastewater samples used in experiments were collected from an industrial chemical plant located in the Jiangsu province in southeast China. The plant engages in the production of chemical intermediates for pharmaceuticals, dyes, and pesticides. The main products are *P*-nitrotoluene (PNT) and *O*-nitrotoluene (ONT). The wastewater samples were taken from the nitration process and nitrobenzene was the major by-product during the process. The characteristics of the wastewater are given in Table 1.

Table 1. Water quality indexes of wastewater used in experiments.

Index	COD (mg/L)	BOD ₅ /COD	TOC (mg/L)	Acute Biotoxicity (mg Zn ²⁺ /L)	Nitrobenzene (mg/L)	pH	Conductivity (μS/cm)
Values	7500–8000	0.1	2000	471–490	>300	1.8	38,000

2.2. Degradation of Chemical Wastewater by the Pyrite Fenton System and the Classic Fenton System

Experiments on the pyrite Fenton and classic Fenton systems were conducted in 250-mL Erlenmeyer flasks. Chemical wastewater (200 mL) and a dosage of natural pyrite (2 g) were mixed, which was calculated to a solid-liquid ratio of 10 g/L, yielding an iron (as Fe(II)) concentration of 2500 mg/L (44.64 mmol/L). The degradation process was initiated by adding 1.02 mL of H₂O₂ (30%) into the flask, yielding an initial concentration of 50 mmol/L H₂O₂, after which the resulting slurry was mixed using a mechanical stirrer (150 rpm) at 25 °C. The classic Fenton system was operated under the same initial

experimental conditions as for the pyrite Fenton system except 44.64 mmol/L of $\text{FeSO}_4 \cdot 7\text{H}_2\text{O}$ was used as an aqueous iron source instead of pyrite. Experiments were conducted at various initial pH (1.8–7), obtained by adding diluted sulphuric acid (10%) or sodium hydroxide solution (5 mol/L). Samples (1 mL) of solution were retrieved from each reaction flask at regular intervals (every 20 min) for further analysis using the techniques described below under “Analytical methods”. Before the measurement of COD, BOD_5 , acute biotoxicity, and the concentration of nitrobenzene and aniline, the pH of samples were adjusted to 8–9 to remove the residual aqueous solution iron and then they were aerated with N_2 for 30 min to remove the residual H_2O_2 . The measurement of the concentration of Fe^{2+} , total aqueous Fe did not adjust the values of pH of samples. All experiments were performed in duplicate.

2.3. Effects of the Dosage of Pyrite and H_2O_2

The effects of the dosage of pyrite and H_2O_2 were investigated in batch experiments. All experiments were performed in Erlenmeyer flasks at 25 °C. To observe the effects of pyrite and H_2O_2 dosages, the pyrite concentrations were set as 5, 10, 20, and 50 g/L, and the H_2O_2 concentrations were set at 1, 2, 5, 10, 50, and 100 mmol/L. All experiments were performed in duplicate.

2.4. Analytical Methods

The COD concentration was measured by COD analyzer (HACH, DRB 200, Loveland, CO, USA), respectively [25]. The BOD_5 was measured by the amount of oxygen consumed by the decomposition of organic matter in wastewater over 5 days [25]. The BOD_5/COD index (B/C) was used to assess the wastewater biodegradability.

The acute biotoxicity measurements were conducted using the widely used photobacterium bioassay. This method quantifies the decrease in light emission of the bioluminescent bacteria *Photobacterium phosphoreum*, which results from exposure to pollutants. The extent of luminescence inhibition after 5 min exposure is standardized into an equivalent concentration of Zn^{2+} , which is used to express the degree of pollutant effects on the test bacteria. Thus, a greater luminescence inhibition corresponds to a higher equivalent Zn^{2+} concentration [26].

The concentration of Fe^{2+} was measured using to the 1,10-phenanthroline method [27]. The total aqueous Fe concentration was determined using flame atomic absorption spectrophotometry. The concentration of nitrobenzene was measured using the reduction azo-photometry [25], and the amount of aniline in the samples was determined using the *N*-(1-Naphthalene)-Ethylenediamine (*N*-(1-naphthalenyl)-1,2-ethanediamine; *N*-na; $\text{C}_{10}\text{H}_7\text{NHCH}_2\text{CH}_2\text{NH}_2$) method according to previous research [28].

All samples with no dilution were used for EEM analysis with Shimadzu UV-1800 ultraviolet-visible (UV/vis) spectrophotometer. The EEM fluorescence spectra were obtained as follows. The scanning field was set at an excitation wavelength from 245 to 400 nm and the emission wavelength from 280 to 500 nm, with 5- and 1-nm sampling intervals in excitation (Ex) and emission (Em) modes, respectively. All fluorescence data were presented in arbitrary units. A PARAFAC analysis was used to interpret the EEM data after first completing several preparative steps (*i.e.*, data loading, scattering removal, and initial explorative data analysis) [29–31].

3. Results and Discussion

3.1. Comparison of COD Removal in the Pyrite Fenton System and the Classic Fenton System

As shown in Figure 1a, at initial wastewater pH of 1.8, approximately 30% of the COD was removed in the pyrite Fenton system within 120 min, whereas only 20% of the COD was removed in the classic Fenton system in the same reaction time. Figure 1b shows that at the optimal initial pH for operation of the classic Fenton process (pH 3 as reported in previous papers [6]), the COD removal efficiency was greater than 30% in both Fenton systems (in 120 min), but the classic Fenton system removed more COD than did the pyrite Fenton system. At an initial pH of 7, the classic Fenton system did not degrade the organics of the wastewater (Figure 1c); in contrast, the COD removal efficiency was still greater than 25% in the pyrite-Fenton system.

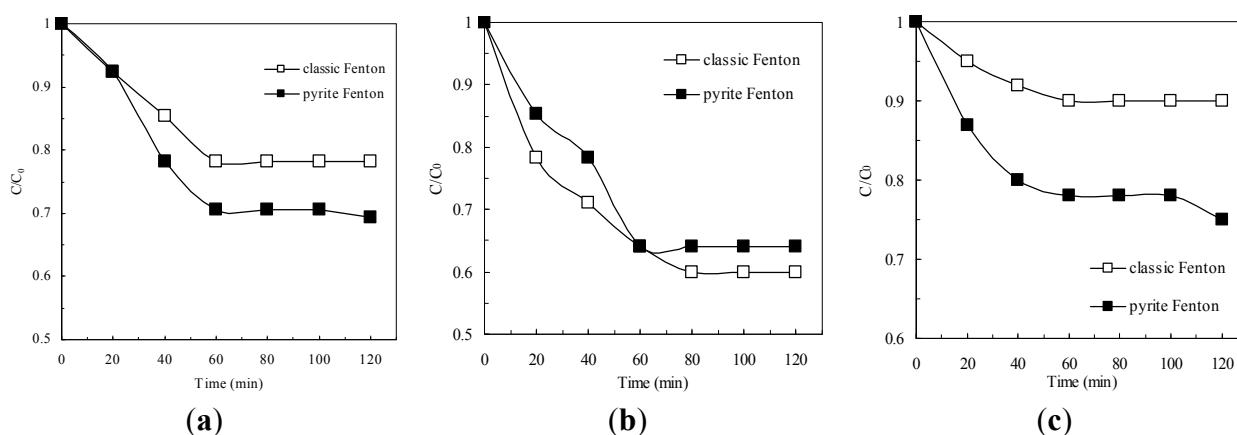
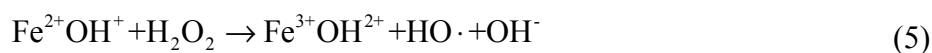
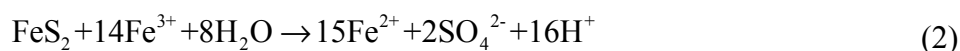
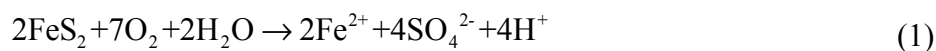


Figure 1. Comparison of pyrite Fenton and classic Fenton for the removal of COD under different initial pH. (a) initial pH = 1.8; (b) initial pH = 3; (c) initial pH = 7. Experimental conditions: (pyrite)₀ = 10 g/L, (H₂O₂)₀ = 50 mmol/L.

These results demonstrated that pyrite has a benefit as Fenton reaction media because the initial pH had little influence on the removal of organics in the pyrite Fenton process. Previous authors reported that two types of oxidation occur during the pyrite Fenton process: pyrite oxidation (Equations (1)–(3)) and Fenton oxidation (Equations (4) and (5)) [21–23].



Mechanisms on the formation of H₂O₂ and HO· by pyrite in oxic aqueous solutions were investigated systematically in previous studies [21–23]. In the presence of oxygen, pyrite can react to produce Fe²⁺ in the solution (Equation (1)), then the aqueous Fe²⁺ reacts with H₂O₂ to form HO· and changes to Fe³⁺ (Equation (4)). Therefore, in the pyrite Fenton system, both the generation of aqueous Fe²⁺ (Equation (1))

and of $\text{HO}\cdot$ (Equation (4)) could be major rate-limiting reactions that affect the removal of wastewater COD. However, in the classic Fenton system, the generation of $\text{HO}\cdot$ (Equation (4)) is the only rate-limiting reaction. As shown in Figure 2, the aqueous total Fe concentration in the pyrite system gradually increased, which indicated that the aqueous Fe^{2+} was generated gradually. When the process was applied at the initial wastewater pH of 1.8, the aqueous total Fe concentration was 725 mg/L after 120 min treatment. In contrast, the aqueous total Fe concentration was only 195 mg/L at an initial wastewater pH of 7, which resulted in less iron sludge being produced. In addition, the less iron concentration could be reduced to 21.2 mg/L after the subsequent coagulation and sedimentation process.

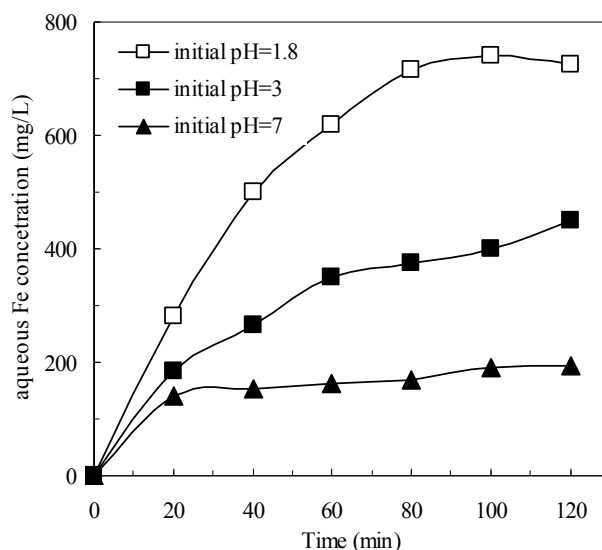


Figure 2. Aqueous Fe concentrations during the degradation in pyrite Fenton systems under different initial pH. Experimental conditions: $(\text{pyrite})_0 = 10 \text{ g/L}$, and $(\text{H}_2\text{O}_2)_0 = 50 \text{ mmol/L}$.

According to Equation (4), the initial pH plays a key role in the removal of organics in the classic Fenton system. To avoid the precipitation of $\text{Fe}(\text{OH})_3$, which consumes Fe^{2+} in the aqueous solution, the classic Fenton process is always operated at pH 3 (or lower) [32,33]. The present study demonstrated the validity of this conclusion. However, in the pyrite Fenton system, the COD removal efficiencies achieved at all initial pH values were quite similar, although the efficiency at pH 3 was somewhat superior to that at the other pH values. This phenomenon can be explained by the following reasons.

As a heterogeneous material, pyrite has the primary advantage of helping to avoid the formation of iron oxide sludge [34]. Thus, pyrite can expand the effective pH range in which the Fenton process can operate successfully [21,23]. The variation of suspension pH with respect to time in the pyrite Fenton system is shown in Figure 3. As the reaction proceeded, the pH of the suspension underwent obvious changes. When the initial wastewater pH was extremely acidic, the pH slightly (within a few minutes) increased as the reaction progressed, then remained in the acidic range. In contrast, when the initial wastewater pH was at neutrality, the pH first decreased drastically from 7 to 5.5, and then gradually decreased to pH 4.8. As described by Equation (1), the pyrite can react with oxygen and generate protons, which is the reason that the pH decreased. Importantly, the decreased pH helped sustain the Fenton reaction. Therefore, in contrast to the classic Fenton system, the pyrite Fenton system can naturally achieve the appropriate pH conditions for effective Fenton reactions without the need for chemical additives.

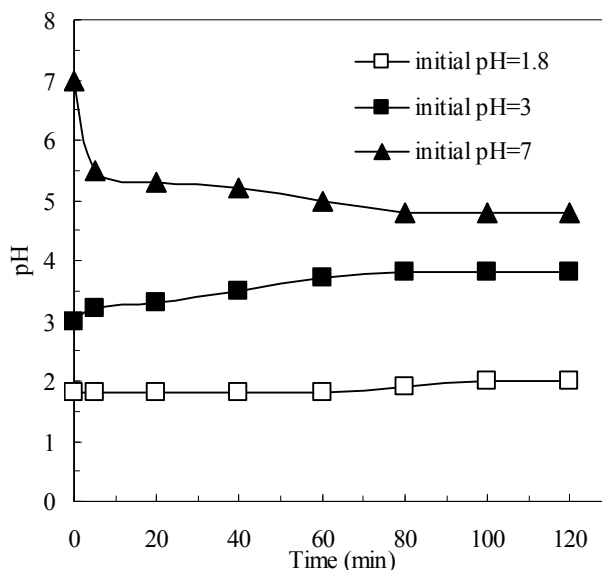


Figure 3. Variation of suspension pH with respect to time. Experimental conditions: $(\text{pyrite})_0 = 10 \text{ g/L}$, and $(\text{H}_2\text{O}_2)_0 = 50 \text{ mmol/L}$.

3.2. Biodegradability Enhancement and Acute Biototoxicity Reduction by the Pyrite Fenton System

To investigate the effect of biodegradability enhancement and acute biototoxicity reduction via different Fenton system, batch experiments using pyrite, zero valent iron, and magnetite were set up. The changes in the biodegradability of wastewater as a result of treatment are illustrated in Figure 4. The B/C index of the untreated chemical wastewater was nearly 0.1, which demonstrated that this kind of wastewater was resistant to treatment using traditional biological technologies. Neither oxidation by H_2O_2 or reduction by natural pyrite as individual processes improved the biodegradability of the wastewater remarkably. The B/C index following H_2O_2 oxidation was 0.11, and was 0.13 following pyrite reduction. However, after wastewater was treated using the Fenton processes, the B/C index increased to approximately 0.3 in the classic Fenton system, to 0.31 in the pyrite Fenton system, and to 0.34 in the ZVI Fenton system, while it was only 0.23 in the magnetite Fenton system. Thus, the pyrite Fenton system showed a remarkable ability to improve wastewater biodegradability.

As shown in Figure 4, the COD efficiency of oxidation by H_2O_2 was 10% within 120 min, however, the value of BOD was decreased, suggesting that the biodegradability enhancement was mainly caused by COD removal. In the pyrite system, the COD was removed less, but the BOD was increased remarkably. The result showed that pyrite has an extremely strong reducing capacity for pollutant removal. The electron-deficient groups of compounds that include nitrobenzene could be reduced to electron-donating groups (such as aniline) to increase the biodegradability of wastewater. Comparing the results of COD removal and biodegradability enhancement of pyrite Fenton system, the biodegradability data demonstrated more remarkable changes than COD removal. These results indicated that the organic compounds were not degraded completely but were transformed to other less toxic compounds. During the Fenton process, the macromolecular compounds were split to small molecule substances by $\text{HO}\cdot$, and these reactions tend to simplify the structure of molecules to improve the biodegradability.

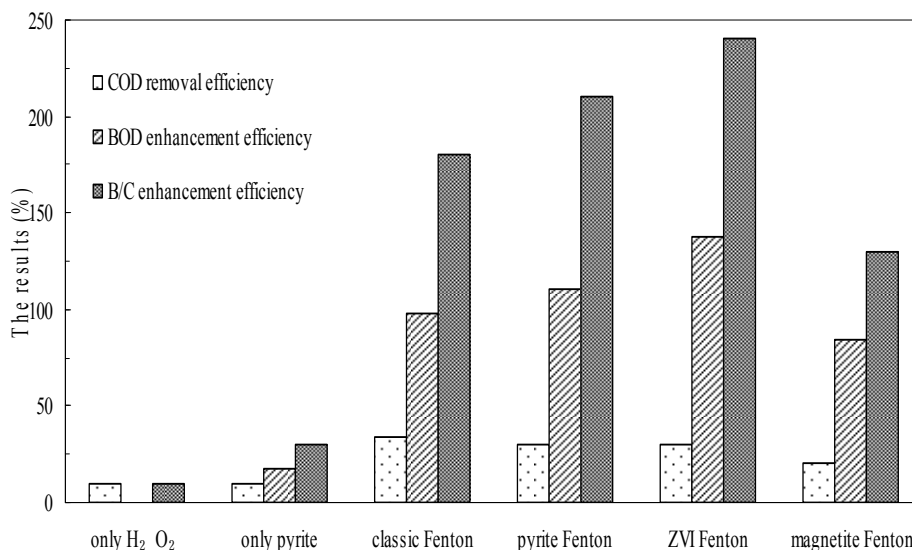


Figure 4. Comparison of pyrite Fenton and classic Fenton for the enhancement of B/C. Experimental conditions: (pyrite)₀ = 10 g/L, (ZVI)₀ = 10 g/L, (magnetite)₀ = 10 g/L, (H₂O₂)₀ = 50 mmol/L, and initial pH = 3.

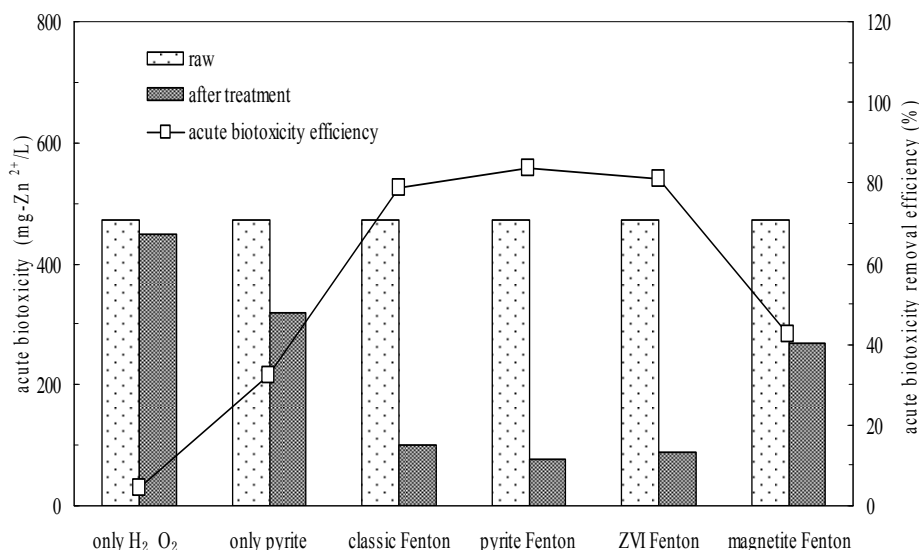


Figure 5. Comparison of pyrite Fenton and classic Fenton for the removal of acute biotoxicity. Experimental conditions: (pyrite)₀ = 10 g/L, (ZVI)₀ = 10 g/L, (magnetite)₀ = 10 g/L, (H₂O₂)₀ = 50 mmol/L, and initial pH = 3.

Batch experiments further confirmed the biotoxicity reduction effected by wastewater treatment. The acute biotoxicity values of the wastewater before and after treatment are shown in Figure 5. The initial overall toxicity of the influent wastewater was 471.4 mg Zn²⁺/L, which indicated that the wastewater posed a high environmental risk. As with their effects on wastewater biodegradability, neither H₂O₂ oxidation nor pyrite reduction acting alone reduced the acute biotoxicity of wastewater observably. The acute biotoxicity values of samples subjected to H₂O₂ oxidation and pyrite reduction were 450 and 320 mg Zn²⁺/L, respectively. However, the acute biotoxicity values of samples were remarkably reduced to 100, 77 and 90 mg Zn²⁺/L after the classic Fenton, pyrite Fenton and ZVI Fenton treatments, respectively. While it was 270 mg Zn²⁺/L in the magnetite Fenton system.

The results indicated that the magnetite Fenton system can not significantly improve the biodegradability and reduce the biotoxicity of chemical wastewater, while both the pyrite Fenton and ZVI Fenton technologies are the novel alternative to the classic Fenton process for simultaneously improving the biodegradability and reducing the biotoxicity.

3.3. Effects of the Pyrite and H_2O_2 on the Removal of Organics in the Pyrite Fenton System

The effect of natural pyrite dosage on the removal of pollutants was examined in batch experiments using different initial dosages of pyrite (0–50 g/L). The results are shown in Figure 6. Within 120 min, the COD removal efficiency reached 10%, 20%, 36%, 32%, and 26% at pyrite dosages of 0, 5, 10, 20, and 50 g/L, respectively. These results indicated that COD removal increased significantly as the initial pyrite concentration increased from 0 g/L to 10 g/L, whereas COD removal decreased slightly as the initial pyrite concentrations increased from 20 g/L to 50 g/L. Based on these results, a pyrite dosage of 10 g/L was optimal for the pyrite Fenton system treating the particular wastewater used in the experiments. This variation in COD removal as a function of pyrite dosage probably can be attributed to the follow reason.

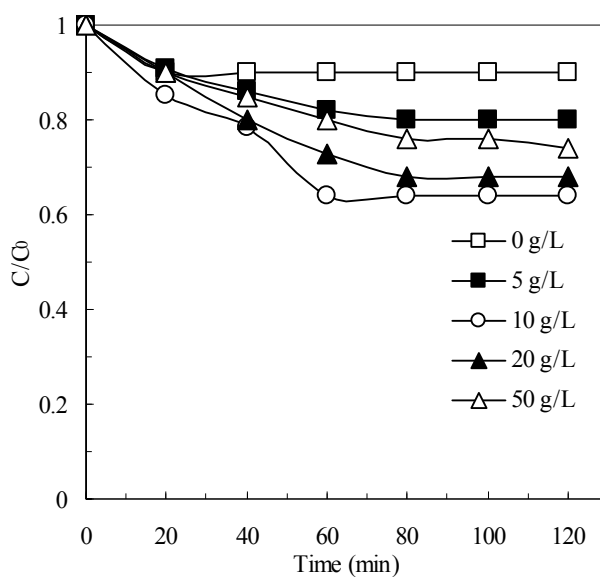


Figure 6. The effect of pyrite dosage on the removal of COD in pyrite Fenton system. Experimental conditions: $(H_2O_2)_0 = 50$ mmol/L, and initial pH = 3.

According to Equations (1)–(3), increasing the amount of pyrite in suspension proportionally increases the aqueous Fe^{2+} concentration, which improves $HO\cdot$ formation (Equation (4)) and enhances the degradation of organics. However, previous authors pointed out that an excessive amount of aqueous Fe^{2+} in a pyrite suspension may promote the unwanted consumption of $HO\cdot$ (as shown in Equation (6)), which can negatively affect the oxidative degradation of COD by Fenton reactions [21,22,32].



Figure 7 shows the effect of the initial H_2O_2 concentrations on the removal of COD in the pyrite Fenton system. When the initial H_2O_2 was 1 mmol/L, the removal efficiency of COD was 15% after 120 min, but at an initial H_2O_2 concentration of 50 mmol/L, this efficiency increased to 36%. However,

the TOC removal efficiency was only 10% under this condition. The results indicated that the organic compounds contained in the wastewater were not degraded completely but were split to small molecule substances by HO·. The stoichiometric amount of H₂O₂ for the complete mineralization of the carbon content to CO₂ and H₂O following Equation (7) was calculated to 33.33 mmol/L. It is clear that the actual dosage of H₂O₂ is more than the calculated value. Segura *et al.* also found this phenomenon in zero valent iron Fenton system [35]. They illustrated that the increase of the H₂O₂ showed a clear enhancement of performance when the highest oxidant loading (200% H₂O₂) was used. However, when the initial H₂O₂ increased to 100 mmol/L, the COD remove efficiency decreased to 30.



These variations were consistent with those observed in previous studies [6,36], which proposed that when an appropriate concentration of Fe²⁺ was provided in the reaction system, an increase of the H₂O₂ concentration could enhance the oxidative degradation of organics in the pyrite Fenton system due to the improvement in HO· formation. In contrast, an excessive amount of H₂O₂ in a pyrite suspension readily reacts with generated HO· (Equation (8)), reducing the oxidative removal of COD by HO·.

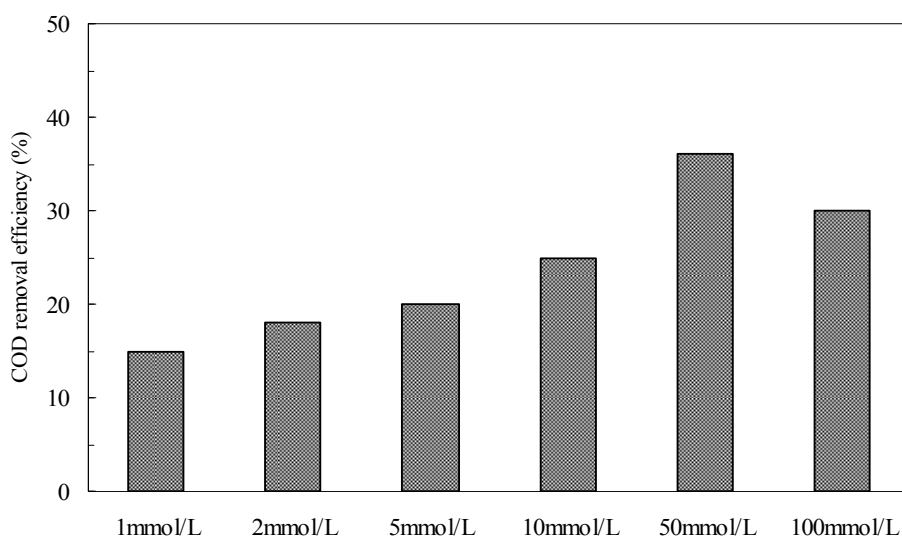


Figure 7. The effect of H₂O₂ concentrations on the removal of COD in pyrite Fenton system. Experimental conditions: (pyrite)₀ = 10 g/L, and initial pH = 3.

However, neither of the potentially negative effects posed by excessive amounts of pyrite and H₂O₂ appeared to be significant in the pyrite Fenton system. Relative insensitivity to such effects was another advantage that the pyrite Fenton system offered over the classic Fenton system.

3.4. The Generation of Aniline in the Pyrite Fenton System

Figure 8 shows the influence of initial H₂O₂ concentration on the generation of aniline. The untreated wastewater did not contain aniline, and no aniline was generated in the classic Fenton process. In the pyrite Fenton system, when only pyrite was added, the concentration of aniline in the treated wastewater was 18.7 mg/L after 120 min, which indicated that the natural pyrite could have a reduction capacity for

nitro-aromatic compounds. In response to H_2O_2 , within 120 min the concentration of aniline reached 23.4, 37.5, 9.4, and 3.7 mg/L at initial H_2O_2 concentrations of 1, 2, 5, and 10 mmol/L, respectively. However, when the initial H_2O_2 concentration was 50 mmol/L, no aniline was detected in the aqueous solution. These results showed that low initial concentrations of H_2O_2 (from 1 mmol/L to 2 mmol/L) significantly improved the reduction performance of pyrite, whereas high concentrations of H_2O_2 (5 mmol/L to 50 mmol/L) inhibited the reduction performance.

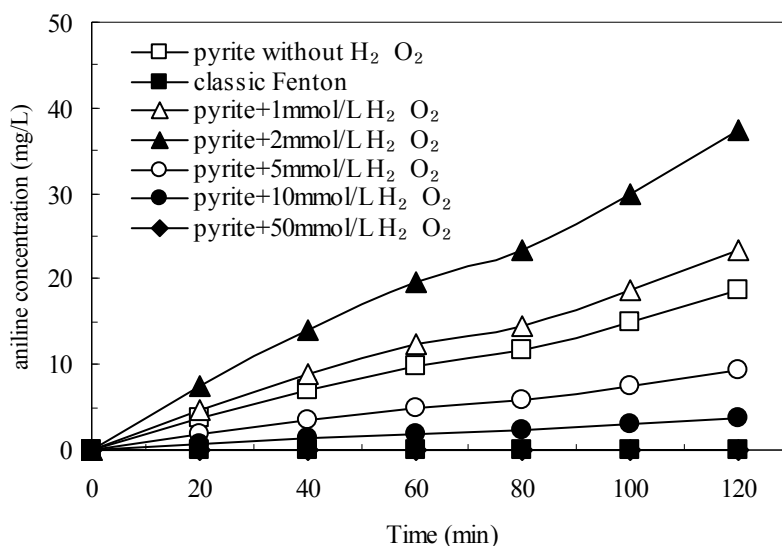


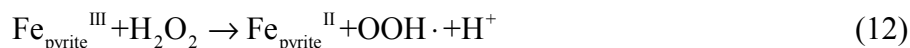
Figure 8. Amount of aniline in the aqueous solution with different initial H_2O_2 concentration. Experimental conditions: $(pyrite)_0 = 10$ g/L, and initial pH = 1.8.

Stumm and James proposed that the dissociation of pyrite releases dissolved ferrous and sulfur (S_2^{2-}) ions, which have an extremely strong reducing capacity for pollutant removal (Equation (9)) [37]. Zhang also found that the released dissolved ferrous effectively made pyrite an electron donor that resulted in the formation of Fe^{3+} , whereas the nitro group of compounds that include nitrobenzene were electron-deficient and thus, they could be readily reduced [34].



Many studies have suggested that the decomposition of H_2O_2 can be controlled by surface-catalyzed process in the heterogeneous reaction involving iron oxides (e.g., magnetite, goethite, and hematite) [38,39]. Kong pointed out that the oxygen and H_2O_2 in an aqueous solution could oxidize the surface Fe(II) of pyrite to Fe(III), as described in Equations (10) and (11) [40]. Kwan found that most organics in the heterogeneous Fenton process were degraded by $HO\cdot$ produced from dissolved Fe^{2+} (Equation (4)), not by a surface-catalyzed process (Equation (10)) [41]. Bae also observed this phenomenon in the pyrite Fenton system and furthermore demonstrated that H_2O_2 could reduce the surface Fe(III) of pyrite to Fe(II), and that the regenerated Fe(II) could be released into the aqueous solution and react with H_2O_2 to produce $HO\cdot$ (Equation (4)), which could react with target contaminants [21].





The pathway of this reaction process is shown in Figure 9. According to Equation (12), H_2O_2 can reduce the surface Fe(III) of pyrite to Fe(II) and enhance the generation of aqueous Fe^{2+} . When the initial concentration of H_2O_2 is low (such as 1 mmol/L and 2 mmol/L), the residual H_2O_2 in the aqueous solution cannot oxidize the aqueous Fe^{2+} thoroughly; hence, there is ample aqueous Fe^{2+} to join in the reduction of nitrobenzene compounds to aniline. In the present study, aqueous Fe^{2+} concentrations reached 198 and 187 mg/L in the pyrite Fenton system (after 120 min) at initial H_2O_2 concentrations of 1 and 2 mmol/L, respectively. However, when the initial H_2O_2 concentration was sufficient (greater than 10 mmol/L), the aqueous Fe^{2+} was oxidized by the excess H_2O_2 , indicating that Fenton oxidation is the main reaction that occurs during the entire process. In fact, the mechanism and entire process of the pyrite Fenton technology is complex and not very explicit. Further investigation of the reductive transformations and oxidative pollutant degradation that occurs in the pyrite Fenton system is ongoing.

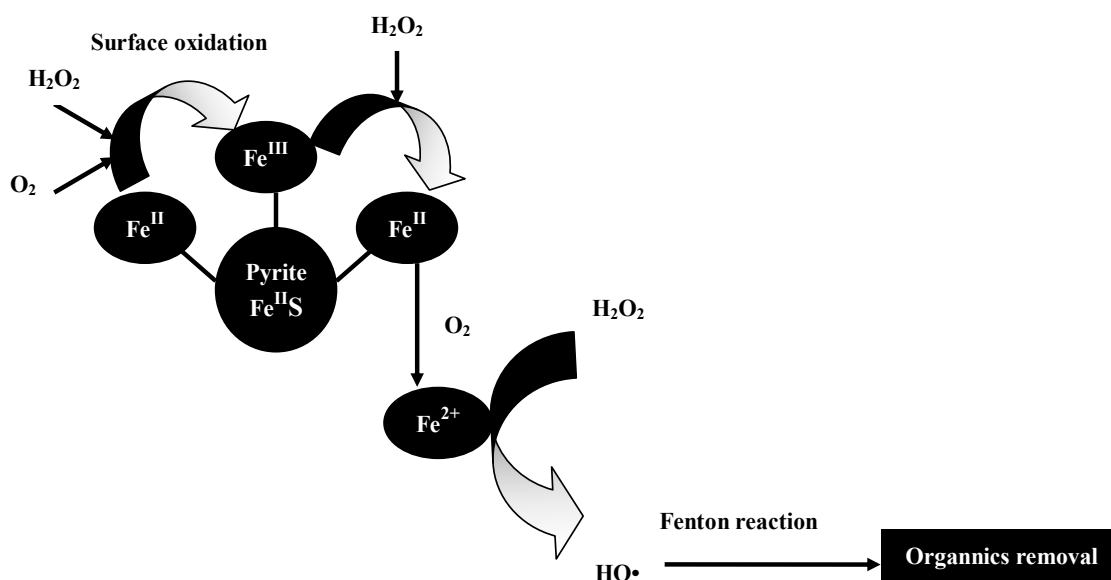


Figure 9. Proposed pathway for oxidative degradation of organics by pyrite Fenton system.

3.5. Evaluation of Organic Functional Groups by EEM in the Pyrite Fenton System

EEM has been frequently used to characterize organics in water and wastewater treatment systems due to its high sensitivity, good selectivity, and non-destructive effect on samples [42,43]. As a technique of multivariate data analysis, PARAFAC can mathematically decompose the complex fluorescence spectra into individual fluorescent components for both quantitative and qualitative analysis [44,45]. In the present study, the EEM-PARAFAC analysis method was used to evaluate the organic functional groups in the wastewater before and after it was subjected to classic Fenton and pyrite Fenton treatment.

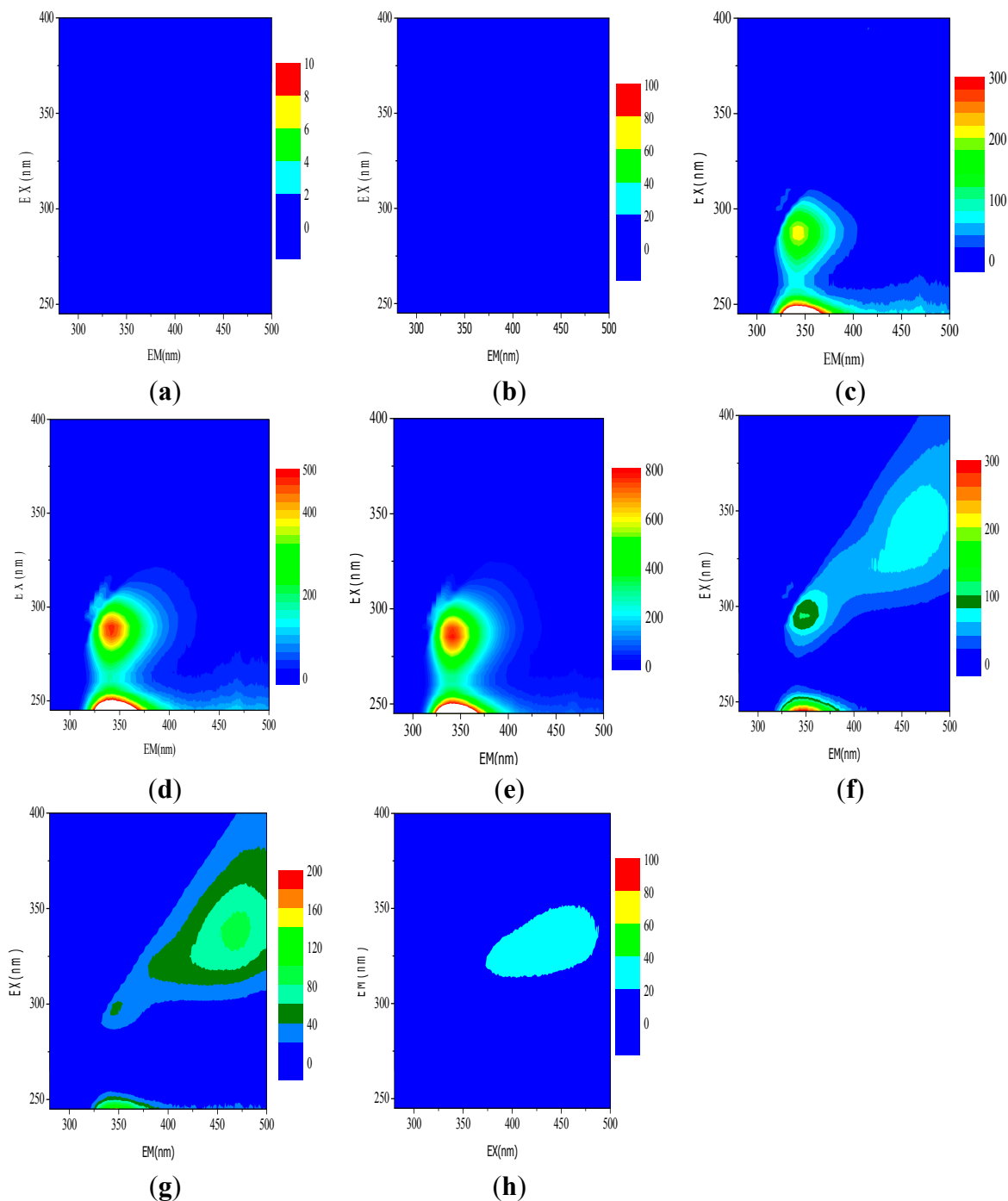


Figure 10. Sample results scanned by three-dimensional fluorescence. (a) raw water; (b) classic Fenton; (c) pyrite without H₂O₂; (d) pyrite + 1 mmol/L H₂O₂; (e) pyrite + 2 mmol/L H₂O₂; (f) pyrite + 5 mmol/L H₂O₂; (g) pyrite + 10 mmol/L H₂O₂; (h) pyrite + 50 mmol/L H₂O₂.

Figure 10 shows the three-dimensional fluorescence spectra for various samples. Using the peak-picking function of the instrument's FL solution software, no peaks were found in the EEM spectra from either the raw (*i.e.*, untreated) wastewater or from wastewater treated using the classic Fenton process (Figure 10a,b); this indicated that there were no electron-donating groups contained in these samples. One major peak was found in the spectra from a number of samples at approximately Ex 290 nm and Em 432 nm (Figure 10c–g). The relative heights of the peaks for each sample were calculated to 211.1, 471.9, 772.2, 102.3, and 41.87, respectively. No spectral peak was observed for the sample

that included pyrite and 50 mmol/L H₂O₂ (Figure 10h). Generally, fluorescent peaks at Ex 290 nm and Em 432 nm originate from amine groups (-NH₂), and the height of a peak corresponds with the quantity of organic material that contains amine groups (such as aniline) [46]. The spectral responses shown in Figure 10 indicated that low initial H₂O₂ concentrations facilitated the reduction of organic molecules containing electron-withdrawing groups (such as -NO₂) to electron-donating groups (such as -NH₂) by pyrite. These results proposed that increased H₂O₂ concentration could enhance the reduction of nitrobenzene in a pyrite Fenton system by improving the surface Fe(II) regeneration.

4. Conclusions

In this research, the treatment of actual chemical wastewater using an enhanced Fenton system catalyzed by natural pyrite was evaluated systematically. The results shows that the Fenton process catalyzed using natural pyrite effectively removes COD across a broad range of initial pH (pH 1.8 to 7). Furthermore, the pyrite Fenton process effectively increases the biodegradability of treated wastewater and simultaneously reduces the toxicity of treated wastewater. Compared to that of the classic Fenton process, the COD removal efficiency of the pyrite Fenton process is less sensitive to the initial solution pH and relatively insensitive to excessive amounts of both pyrite and H₂O₂. Finally, in the pyrite Fenton system, the reduction of nitrobenzene and organic molecules containing electron-withdrawing groups to electron-donating groups by natural pyrite can be promoted by adding a small amount of H₂O₂ (initial concentration <5 mmol/L). Thus, the pyrite Fenton process offers several operational advantages over the classic Fenton process and is a viable method by which to remediate organic pollutants in wastewater, while providing an environmentally friendly alternative for reusing natural pyrite.

Acknowledgments

We gratefully acknowledge the generous support provided by the Nation Water Pollution Control and Management of major special science and technology of China (No. 2015ZX07204002) and the National Natural Science Foundation of China (NO. 51408295), China.

Author Contributions

All authors were involved in discussing the ideas and designing this study. Sun Liang drafted the manuscript. Li Yan and Li Aimin edited draft versions and finalized the manuscript. All the authors have read and approved the final manuscript.

Conflicts of Interest

The authors declare no conflict of interest.

References

1. Fan, J.H.; Ma, L.M. The pretreatment by the Fe-Cu process for enhancing biological degradability of the mixed wastewater. *J. Hazard. Mater.* **2009**, *164*, 1392–1397.
2. Sun, L.; Wang, C.; Ji, M.; Kong, X. Treatment of mixed chemical wastewater and the agglomeration mechanism via an internal electrolysis filter. *Chem. Eng. J.* **2013**, *215–216*, 50–56.

3. Wu, C.Y.; Zhou, Y.X.; Wang, P.C.; Guo, S.J. Improving hydrolysis acidification by limited aeration in the pretreatment of petrochemical wastewater. *Bioresour. Technol.* **2015**, *194*, 256–262.
4. Ren, C.X.; Li, Y.M.; Li, J.F.; Sheng, G.D.; Hu, L.J.; Zheng, X.M. Immobilization of nanoscale zero valent iron on organobentonite for accelerated reduction of nitrobenzene. *J. Chem. Technol. Biotechnol.* **2014**, *89*, 1961–1966.
5. Yin, W.Z.; Wu, J.H.; Huang, W.L.; Wei, C.H. Enhanced nitrobenzene removal and column longevity by coupled abiotic and biotic processes in zero-valent iron column. *Chem. Eng. J.* **2015**, *259*, 417–423.
6. Chamarro, E.; Marco, A.; Esplugas, E. Use of Fenton reagent to improve organic chemical biodegradability. *Water Res.* **2001**, *35*, 1047–1051.
7. Canizares, P.; Paz, R.; Saez, C.; Rodrigo, M.A. Costs of the electrochemical oxidation of wastewaters: A comparison with ozonation and Fenton oxidation processes. *J. Environ. Manag.* **2009**, *90*, 410–420.
8. Dariush, S.; Moheb A.; Abbas R.; Larouk S.; Roy R.; Azzouz A. Total mineralization of sulfamethoxazole and aromatic pollutants through Fe(2+)-montmorillonite catalyzed ozonation. *J. Hazard. Mater.* **2015**, *298*, 338–350.
9. Nakai, S.; Okuda, T.; Okada, M. Production of mono- and di-carboxylated polyethylene glycols as a factor obstacle to the successful ozonation-assisted biodegradation of ethoxylated compounds. *Chemosphere* **2015**, *136*, 153–159.
10. Kaur, M.; Verma, A.; Rajput, H. Potential use of foundry sand as heterogeneous catalyst in solar photo-fenton degradation of herbicide isoproturon. *Int. J. Environ. Res.* **2015**, *9*, 85–92.
11. Doumic, L.I.; Soares, P.A.; Ayude, M.A.; Cassanello, M.; Boaventura, R.A.R.; Vilar, V.J.P. Enhancement of a solar photo-Fenton reaction by using ferrioxalate complexes for the treatment of a synthetic cotton-textile dyeing wastewater. *Chem. Eng. J.* **2015**, *277*, 86–96.
12. Che, H.; Lee, W. Selective redox degradation of chlorinated aliphatic compounds by Fenton reaction in pyrite suspension. *Chemosphere* **2011**, *82*, 1103–1108.
13. Huang, R.; Fang, Z.; Yan, X.; Cheng, W. Heterogeneous sono-Fenton catalytic degradation of bisphenol A by Fe₃O₄ magnetic nanoparticles under neutral condition. *Chem. Eng. J.* **2012**, *197*, 242–249.
14. Masomboon, N.; Ratanatamskul, C.; Lu, M.C. Chemical oxidation of 2,6-dimethylaniline in the Fenton process. *Environ. Sci. Technol.* **2009**, *43*, 8629–8634.
15. Matta, R.; Hanna, K.; Chiron, S. Fenton-like oxidation of 2,4,6-trinitrotoluene using different iron minerals. *Sci. Total. Environ.* **2007**, *385*, 242–251.
16. Maria, A.F.D.; Emilio, R.; María, F.F.; Marta, P.; Maria, Á.S. Degradation of organic pollutants by heterogeneous electro-Fenton process using Mn-alginate composite. *J. Chem. Technol. Biotechnol.* **2015**, *90*, 1439–1447.
17. Hu, X.B.; Deng, Y.H.; Gao, Z.Q.; Liu, B.Z.; Sun, C. Transformation and reduction of androgenic activity of 17 alpha-methyltestosterone in Fe₃O₄/MWCNTs-H₂O₂ system. *Appl. Catal. B-Environ.* **2012**, *127*, 167–174.
18. Todd, E. Surface oxidation of pyrite under ambient atmospheric and aqueous (pH = 2 to 10) conditions: Electronic structure and mineralogy from X-ray absorption spectroscopy. *Geochim. Cosmochim. Acta* **2003**, *67*, 881–893.

19. Arienzo, M. Oxidizing 2,4,6-trinitrofluorene with pyrite-H₂O₂ suspensions. *Chemosphere* **1999**, *39*, 1629–1638.
20. Che, H.; Bae, S.; Lee, W. Degradation of trichloroethylene by Fenton reaction in pyrite suspension. *J. Hazard. Mater.* **2011**, *185*, 1355–1361.
21. Bae, S.; Kim, D.; Lee, W. Degradation of diclofenac by pyrite catalyzed Fenton oxidation. *Appl. Catal. B-Environ.* **2013**, *134*, 93–102.
22. Wu, D.L.; Feng, Y.; Ma, L.M. Oxidation of Azo Dyes by H₂O₂ in presence of natural pyrite. *Water Air Soil. Pollut.* **2013**, *224*, doi:10.1007/s11270-012-1407-y.
23. Zhang, Y.L.; Zhang, K.; Dai, C.M.; Zhou, X.F.; Si, H.P. An enhanced Fenton reaction catalyzed by natural heterogeneous pyrite for nitrobenzene degradation in an aqueous solution. *Chem. Eng. J.* **2014**, *244*, 438–445.
24. Wang, C.; Xi, J.Y.; Hu, H.Y. Chemical identification and acute biotoxicity assessment of gaseous chlorobenzene photodegradation products. *Chemosphere* **2008**, *73*, 1167–1171.
25. APHA; AWWA; WEF. *Standard Methods for the Examination of Water and Wastewater*, 20th ed.; APHA/AWWA/WEF: Washington, DC, USA, 1998.
26. Wang, L.S.; Wei, D.B.; Wei, J.; Hu, H.Y. Screening and estimating of toxicity formation with photobacterium bioassay during chlorine disinfection of wastewater. *J. Hazard. Mater.* **2007**, *141*, 289–294.
27. Stookey, L.L. Ferrozine—A new spectrophotometric reagent for iron. *Anal. Chem.* **1970**, *42*, 779–781.
28. Norwitz, G.; Keliher, P.N. Spectrophotometric determination of aniline by the diazotization-coupling method with *N*-(1-naphthyl) ethylenediamine as the coupling agent. *Anal. Chem.* **1981**, *53*, 1238–1240.
29. Stedmon, C.A.; Bro, R. Characterizing dissolved organic matter fluorescence with parallel factor analysis: A tutorial. *Limnol. Oceanogr. Methods* **2008**, *6*, 572–579.
30. Bagtho, S.A.; Sharma, S.K.; Amy, G.L. Tracking natural organic matter (NOM) in a drinking water treatment plant using fluorescence excitation—Emission matrices and PARAFAC. *Water Res.* **2011**, *45*, 797–809.
31. Li, W.T.; Chen, S.Y.; Xu, Z.X.; Li, Y.; Shuang, C.D.; Li, A.M. Characterization of dissolved organic matter in municipal wastewater using fluorescence PARAFAC analysis and chromatography multi-excitation/emission scan: A comparative study. *Environ. Sci. Technol.* **2014**, *48*, 2603–2609.
32. Pignatello, J.J.; Oliveros, E.; MacKay, A. Advanced oxidation processes for organic contaminant destruction based on the Fenton reaction and related chemistry. *Crit. Rev. Environ. Sci. Technol.* **2006**, *36*, 1–84.
33. Hashemian, S.; Tabatabaee, M.; Gafari, M. Fenton oxidation of methyl violet in aqueous solution. *J. Chem.* **2013**, *2013*, doi:10.1155/2013/509097.
34. Zhang, Y.L.; Zhang, K.; Dai, C.M.; Zhou, X.F. Performance and mechanism of pyrite for nitrobenzene removal in aqueous solution. *Chem. Eng. Sci.* **2014**, *111*, 135–141.
35. Segura, Y.; Martínez, F.; Melero, J.A.; Fierro, J.L.G. Zero valent iron (ZVI) mediated Fenton degradation of industrial wastewater: Treatment performance and characterization of final composites. *Chem. Eng. J.* **2015**, *269*, 298–305.

36. Moffett, J.W.; Zika, R.G. Reaction kinetics of hydrogen peroxide with copper and iron in seawater. *Environ. Sci. Technol.* **1987**, *21*, 804–810.
37. Stumm, W.; James, J. *Aquatic Chemistry. An Introduction Empha—Sizing Chemical Equilibria in Natural Waters*; John Wiley & Sons: Michigan, MI, USA, 1981.
38. Pham, A.L.T.; Lee, C.; Doyle, F.M.; Sedlak, D.L. A silica-supported iron oxide catalyst capable of activating hydrogen peroxide at neutral pH values. *Environ. Sci. Technol.* **2009**, *43*, 8930–8935.
39. Xue, X.X.; Hanna, K.; Abdelmoula, M.; Deng, N. Adsorption and oxidation of PCP on the surface of magnetite: Kinetic experiments and spectroscopic investigations. *Appl. Catal. B-Environ.* **2009**, *89*, 432–440.
40. Kong, L.H.; Hu, X.Y.; He, M.C. Mechanisms of Sb(III) oxidation by pyrite-induced hydroxyl radicals and hydrogen peroxide. *Environ. Sci. Technol.* **2015**, *49*, 3499–3505.
41. Kwan, W.P.; Voelker, B.M. Decomposition of hydrogen peroxide and organic compounds in the presence of dissolved iron and ferrihydrite. *Environ. Sci. Technol.* **2002**, *36*, 1467–1476.
42. Westerhoff, P.; Chen, W.; Esparza, M. Fluorescence analysis of a standard fulvic acid and tertiary treated wastewater. *J. Environ. Qual.* **2001**, *30*, 2037–2046.
43. Goldman, J.H.; Rounds, S.A.; Needoba, J.A. Applications of fluorescence spectroscopy for predicting percent wastewater in an urban stream. *Environ. Sci. Technol.* **2012**, *46*, 4374–4381.
44. Stedmon, C.A.; Markager, S.; Bro, R. Tracing dissolved organic matter in aquatic environments using a new approach to fluorescence spectroscopy. *Mar. Chem.* **2003**, *82*, 239–254.
45. Bro, R. The N-Way On-Line Course on PARAFAC and PLS. Available online: <http://www.models.life.ku.dk/~pih/parafac/chap0contents.htm> (accessed on 21 June 2010).
46. Lei, Y.Q.; Wang, G.H.; Guo, P.R.; Li, G.B.; Cai, D.C. The application of three-dimensional fluorescence spectroscopy in the electrochemical degradation of organic pollutions. *Chin. J. Anal. Lab.* **2014**, *33*, 373–376. (In Chinese).